Identification of silibinin and isotretinoin as potent up-regulators of *sFRP4* (Wnt antagonist): *In silico* prediction and *in vitro* validation in breast cancer

Rehana Ramzan[1], Shazia Anwer Bukhari[1]*, Azhar Rasul[2]

1 Department of Biochemistry, Government College University, Faisalabad, Pakistan, **2** Department of Zoology, Baba Guru Nanak University, Nankana Sahib, Pakistan

* shaziabukhari@gcuf.edu.pk

Abstract

Secreted frizzled-related protein 4 (*sFRP4*) plays a fundamental role in the regulation of Wnt signalling, which is crucial for cellular proliferation and differentiation. The *sFRP4* has garnered significant interest as a therapeutic target for metabolic diseases and cancer due to its mechanism of action. Although existing sFRP4 modulators show limited specificity and notable off-target effects, our study explores the potential of known bioactive compounds as more selective and less toxic alternatives. This study is based on the analysis of expression profiles, which demonstrated that the *sFRP4* gene exhibits aberrant expression in multiple cancers, including breast cancer. The protein's primary involvement in cancer signaling pathways was determined through pathway enrichment analysis. The study employed molecular docking analyses and MD simulations to identify breast cancer-fighting small molecules with docking energies of less than −6 kcal/mol, targeting the sFRP4 binding hotspot using 100 natural or synthetic small molecules. Out of 100 screened compounds, Silibinin and Isotretinoin were selected based on docking results and further validated in vitro. In vitro investigations were carried out using the colorimetric MTT assay to assess cell viability and cytotoxicity based on metabolic activity. The potential of Silibinin and isotretinoin to upregulate the tumour suppressor *sFRP4* was further examined using ELISA and real-time quantitative PCR. Our study identified potential compounds for high-potential drug candidates against *sFRP4*, demonstrating their effectiveness in cancer cell death and upregulating *sFRP4* expression through improved drug design methods and experimental studies. In conclusion, our in-silico findings could facilitate the discovery of potential therapeutic agents against breast cancer. Silibinin and Isotretinoin impede cancer cell development in vitro; nonetheless, this study demonstrated that they directly upregulate *sFRP4* and induce apoptosis in breast cancer cells.

Introduction

Breast cancer (BC) is one of the most common cancers worldwide, and its prevalence has been growing for decades. BC was the second most prevalent and fatal disease worldwide in 2022, contributing to 11.6% of new cases and 6.9% of cancer deaths. It was the most frequent cancer in women, contributing to one-sixth of global female cancer fatalities and one-fourth of diagnoses. Although it predominantly affects women (>99% of cases), its occurrence in men is extremely rare. The advancement and evolution of breast cancer are contingent upon genetic anomalies and hormonal dysregulation [1]. Breast cancer is a major source of mortality for women in low- and middle-income nations, where its impact is especially pronounced among these populations [2,3].

Breast cancer incidence is highest following menopause. A number of pathophysiological variables contribute to the onset of breast cancer, including gene mutations, particularly in the BRCA1 and BRCA2 genes, inherited genetic predispositions, hormonal exposure (oestrogen and progesterone), dietary influences, environmental exposure to carcinogenic chemicals, and unhealthy lifestyle choices [4–6]. Potential therapeutic targets in malignancies and reproductive system disorders include a range of proteins, enzymes, vascular endothelial and epidermal growth factor receptor [7–10].

Secreted Frizzled-related protein 4 (*sFRP4*) modulates Wnt signalling extracellularly via binding to the Wnt ligand and frizzled receptor. Therefore, it works as a Wnt ligand antagonist, blocking receptor interaction. *sFRP4* is the largest *sFRP* protein, weighing 39.9 kDa and containing 346 amino acids [11]. In several malignancies, diminished or eliminated expression leads to increased Wnt/β-catenin signaling and excessive cell proliferation [12,13]. Wnt pathway activation is another consequence of *sFRP4* gene silencing or reduced protein production. The first exon of *sFRP4* is flanked by numerous CpG islands. One of the ways genes are silenced, leading to a susceptibility to cancer, is via hypermethylation [14,15]. Restoring *sFRP4* expression presents a favourable therapeutic approach for mitigating breast cancer progression.

Bioactive phytocompounds with antioxidant, anti-inflammatory, and anti-proliferative effects have recently gained attention as potential cancer treatments. These natural compounds provide potential benefits compared to traditional medicines by inducing cytotoxic effects on cancer cells while reducing harm to normal cells. Our strategy involves screening a library of such compounds, including well-documented flavonolignans and retinoids known for their general anticancer properties, to identify specific modulators of sFRP4 [16,17]. Additionally, it modulates key signalling pathways involved in tumour progression [16]. These phytochemicals may provide a synergistic approach in targeting triple-negative breast cancer (TNBC), offering a potentially effective therapeutic strategy.

The drug development process begins with bioinformatics analysis, focusing on identifying effective drugs for treating clinical diseases. This involves identifying biological targets, such as proteins, genes, and RNA, using techniques like molecular docking, ADMET profiling, and three-dimensional structural modelling [18]. Identifying new chemicals that can upregulate the *sFRP4* (Wnt antagonist) is crucial for the

biological development of drugs. This work utilised the PubChem database as the essential resource for screening compounds for drug development within the biological system [19,20]. An effective upregulator of the *sFRP4* target was found in our work by combining molecular docking with MD simulation methods. From an initial virtual screening of 100 bioactive compounds retrieved from databases, Silibinin and Isotretinoin were identified as the most promising candidates based on their most favourable docking scores, positive ADMET properties, and literature-supported anticancer activity.

This research seeks to find an upregulator of *sFRP4* using *in-silico* and *in-vitro* methodologies. Screening, different databases utilising the *sFRP4* target protein, investigation of diverse in-silico methodologies for modulating the molecular pathways linked to the progression of breast cancer, and the molecule's confirmation in in vitro experiments.

Methods

This study combines *in silico* and *in vitro* approaches to identify potential upregulators of sFRP4 in breast cancer. Computational analyses included gene expression profiling, ADMET predictions, molecular docking, and MD simulations, while experimental validation involved MTT assay, wound healing, ELISA, and qPCR.

In silico studies

Survival analysis and gene expression. Breast cancer patients' *sFRP4* expression levels were measured using the UALCAN portal (https://ualcan.path.uab.edu/). The target genes were explored using the Cancer Genome Atlas (TCGA) database, first for invasive breast cancer and then for numerous cancer types. The Kaplan-Meier survival study analysed cancer progression survival.

Gene set enrichment analysis. The gene set enrichment analysis for s*FRP4* was performed using Enricher (https://maayanlab.cloud/Enrichr/). Enrichr serves as a primary resource for performing enrichment analysis of mammalian gene sets. Using databases like KEGG, GO, and Reactome, as well as others that pertain to illnesses, biological processes, and recognized functions, it compares the given gene to a library of annotated genes. This tool may help understand target gene pathways.

Protein structure prediction and validation. As reported by Rehman et al. [21] that no complete experimentally resolved structure of human sFRP4 was available in the Protein Data Bank (PDB), so the 3D structure was predicted using SWISS-MODEL based on homology modelling principles [22]. The resulting model was refined using GalaxyRefine, and the quality of the refined structure was evaluated using multiple bioinformatics tools, including ProSA, PDBsum, ERRAT, and Verify 3D [23–25]. These validation tools confirmed the stereochemical quality, residue environment compatibility, and non-bonded interaction quality of the model, making it suitable for downstream molecular docking analysis. Protein 3D structure prediction and validation were performed using the approach proposed by Rehman et al [21]. The predicted structure was evaluated through multiple bioinformatics tools, ensuring its accuracy and stability. Molecular docking and dynamic simulations confirmed the fidelity of the simulated protein-ligand interactions [26].

Database preparation for bioactive conformation. A focused compound library was developed, consisting of natural phytochemicals and plant-derived bioactive molecules with reported anticancer and chemopreventive activities. These compounds were selected based on a literature search using academic databases including PubChem, Google Scholar, and Science Direct [27,28]. The compounds were selected based on reported or computationally predicted anticancer activity. Additional filters included drug-likeness (Lipinski's Rule of Five) and favourable ADMET properties to ensure pharmacological relevance and safety. The selected ligands were retrieved from PubChem in SDF format, converted into three-dimensional structures using Progenesis SDF Studio, and exported in PDB format for downstream docking analyses [29]. These energy-minimized ligands were then utilized as input files in molecular docking simulations performed with AutoDock Vina to evaluate their binding affinity with the sFRP4 protein target [30].

Biological properties analysis. Using Lipinski's rule of five and pharmacokinetic profiles, each of the top compounds' drug-likeness was evaluated using an in-silico analytical method [31,32]. The most favourable results were evaluated for ADMET qualities utilising SwissADME [33], ADMET lab 3.0 [34], ProTox-II [35], pkCSM [36,37], and admetSAR [38].

Prediction of the active site and preparation of the target protein. An active pocket of the sFRP4 protein was predicted and the detection tool DoGSiteScorer. After manually examining the six predicted active pockets, we finally chose and proceeded with Active Pocket 1 as described previously [21,39,40]. Before docking, PyRx facilitated the import of the protein's energy-minimized PDB structure, its conversion to PDBQT format, and choosing it as the target macromolecule [41,42].

Molecular docking. To dock the *sFRP4* protein with several phytochemical ligands, the Auto Dock Vina run function of PyRx's virtual screening program was used [37,43]. AutoDock Vina evaluates the binding affinity of the ligand with the desired protein using an empirical scoring approach. This empirical scoring formula served as the basis for calculating binding affinities. PyRx now contains input PDB files for ligands and targets. The binding site of the protein that was identified by the DoGSiteScorer was determined by the grid box centre and size measurements. The grid box's size was set at 25.08 Å, y = 19.02 Å, and z = 25.0 Å, while the center's dimensions were set at x = 26.11, y = −9.14, and z = 57.33 [44]. PyRx begins docking using Auto Dock Vina, producing many poses of the ligand attaching to the protein. The binding affinities of these poses are used to rank them. PyRx gives ligand-receptor interaction docking binding energies in kcal/mol. For active medications, a potential binding dock energy of −6 kcal/mol is frequently regarded as a threshold.

Study of ligand interactions. Each phytochemical produced distinct effects after docking. The position with the zero RMSD value and the highest negative binding energy was chosen [38]. Using BIOVIA Discovery Studio, the Autodock-generated protein-ligand interaction findings were examined and displayed [45,46], Snapshots were taken of the best interaction poses. The study utilized BIOVIA Discovery Studio to analyse binding profiles and orientations of proteins' active sites, utilizing energy dynamics of ligands for interaction analysis [47]. The study identifies non-covalent interactions in ligand conformations, including hydrogen bonds and hydrophobic contacts, and selects compounds for further research based on hydrogen bonding docking value [48]. This information may facilitate the creation of more efficacious pharmaceuticals by comprehending their behaviour under varying settings [49].

Targeted molecular dynamics (TMD) simulations. For simulation investigations, the Desmond/Maestro (2022.1 version) was utilized [50,51]. The Protein Preparation Wizard of the Maestro interface was used in order to modify and pre-process the receptor-ligand complexes. The system was also constructed using the System Builder tool. The docked complexes were solvated in an orthorhombic simulation box using the TIP3P explicit water model. Counter-ions were added to neutralize the system, and the setup was then subjected to energy minimization and equilibration prior to the production MD run.

The Desmond software's interaction diagram feature was used to study RMSF, how ligands twist, and the interactions between proteins and ligands, with the RMSD calculated as shown.

$$RMSDx = \sqrt{1/N \sum_{i=1}^{N} \left\langle (r'_1(t_x)) - (r_i(t_{ref}))^2 \right\rangle}$$

(1)

where N is the number of atoms in the atom selection; t ref is the reference time, (typically the first frame is used as the reference and it is regarded as time t = 0); and r' is the position of the selected atoms in frame x after superimposing on the reference frame, where frame x is recorded at time t x. The procedure is repeated for every frame in the simulation trajectory. All TMD simulations were performed in triplicate under identical conditions to ensure reproducibility and consistency of ligand-induced conformational behaviour.

The Root Mean Square Fluctuation (RMSF) is useful for characterizing local changes along the protein chain. The RMSF for residue i is:

$$RMSF_i = \sqrt{1/T \sum_{i=1}^{N} \langle (r'_1(t)) - (r_i(t_{ref}))^2 \rangle}$$

(2)

where T is the trajectory time over which the RMSF is calculated, t ref is the reference time, r i is the position of residue i; r' is the position of atoms in residue i after superposition on the reference, and the angle brackets indicate that the average of the square distance is taken over the selection of atoms in the residue.

Biological evaluation (in-vitro studies)

Cell culture. Triple-negative breast cancer (TNBC) cell line MDA-MB-231 was acquired from the NIBGE Cell Culture Collection. Cells were grown in DMEM with 10% FBS, 1% Penicillin-Streptomycin (100 IU/mL penicillin and 100 µg/mL streptomycin), 2 mM L-glutamine, and 1% NEAAs. Cells were cultured in tissue culture flasks at 37°C in a humidified 5% CO_2 environment. The cells were subcultured at a 1:3 split ratio and treated with 1–2 ml of a 0.25% trypsin-EDTA solution every three to five days.

MTT cell proliferation assay. We used the MTT assay to evaluate anticancer efficacy and ascertain cell viability. At a density of 0.01 x 10⁶ cells/mL, MDA-MB-231 cells were seeded into a 96-well plate with 100 µL supplied to every well. After an overnight incubation period, the medium used for cell growth was removed, and the anticancer medication Silibinin was dissolved suitably before being administered to the cells with immediate effect. The cells were subjected to treatment with Silibinin and isotretinoin throughout a broad spectrum of concentrations (6.25−200 µg/ml). After a treatment period of 72 hours, 10 microliters of MTT (12 mM) reagent, with a reference number of V13154 and a lot number of 1753469, was administered to each well. Life Technologies in Carlsbad, California, United States, manufactured the reagent. Any morphological changes in the cells were seen using an inverted phase contrast microscope (IMT-2; Olympus, Tokyo, Japan), before the MTT reagent was added. The cells spent four hours. After the incubation period, formazan crystals were dissolved by adding 100 µL of DMSO; thereafter, the culture medium was gently removed from every well. The absorbance of every sample at 570 nm was then measured using a Synergy H1 hybrid multi-mode microplate reader (BioTek Instruments Inc., Winooski, VT, USA). Cell viability was determined using the accompanying formula:

$$\%[100 \times (Sample\ Absorption / Control\ Absorption)]$$

The IC50 of cells treated with Silibinin and isotretinoin was determined using Prism (Graphpad Software, Inc., San Diego, CA).

Wound healing assay. Cells were cultured in six-well plates and maintained at 37°C until achieving 80% confluence. The cells were spread out in a single layer and then scraped using a 200 µL autoclaved pipette tip. We shall rinse the cells with PBS after removing the medium. New DMEM with the specified amounts of Silibinin and isotretinoin was introduced to the cells for 0 and 24 hours. A microscope was used to examine and photograph the scraped wound (Olympus IMT-2 Inverted Microscope).

Quantification of *sFRP4* in the supernatants by ELISA.. The concentrations of *sFRP4* were quantified with ELISA kits from Glory Science Co., Ltd (GSCIENCE, CATALOG#: G9233, China, Hong Kong) per the manufacturer's instructions.

Quantitative real-time polymerase chain reaction (qPCR). Under a density of 2 x 105 cells/mL, T25 ultra-low flasks housed MDA-MB-231 cells. To extract RNA, the TRI reagent (Catalog No. 155960, Thermo, USA) was applied to the cells following 48 hours of treatment in DMEM. Following the manufacturer's procedure, cDNA from the extracted RNA was synthesised using the SuperScript III first-strand cDNA synthesis kit (Cat No. 18080051, Life Technologies). Maxima SYBR Green/ROX qPCR Master Mix (2X) was used to amplify the cDNA in a real-time PCR cycler. We used the delta-delta CT technique to quantify the expression after normalizing the data to GAPDH. The data was analysed using GraphPad Prism software. Table 1 presents the entire sequences of the primers utilised by [52].

Statistical analyses

The statistical analyses were carried out in GraphPad Prism 8.0 using a One-way ANOVA. The mean ± standard deviation is used to communicate the results. The p-value was taken to be significant when it was ≤ 0.05.

Table 1. The list of primers used to study the expression profile of the indicated gene.

Name	Forward primer	Reverse primer	Base pair	Accession No.
GAPDH	5'-GGAGTCCCCATCCCAACTCA −3	5'-GCCCATAACCCCCACAACAC −3'	173	XM_063276786.1
sFRP-4	5'AGGCAATAGTCACTGACCTTCC-3'	5'CCTTTTTGCACTTGCACCGAT-3'	129	XM_017592435.1

https://doi.org/10.1371/journal.pone.0331735.t001

Results

Aberrant expression of *sFRP4* in various cancers, including TNBC

Transcripts per million (TPM) scores were used to quantify mRNA levels in tumorous cells compared to normal cells, allowing us to estimate the expression level of these putative target proteins. Access to clinical patient data is made possible via the UALCAN gateway by use of the TCGA database. The investigation started with the assessment of *sFRP4* expression levels in BC patients relative to normal breast tissue. According to Fig 1A, *sFRP4* expression is much higher in healthy individuals compared to those with invasive breast cancer. Compared to normal breast tissue, initial tumours had a much lower median expression of *sFRP4*. This suggests that *sFRP4* is downregulated in BC compared to normal tissue. Since sFRP4 is a known antagonist of the Wnt signalling pathway, its reduced expression in tumours suggests that loss of *sFRP4* may contribute to Wnt pathway activation, which is linked to cancer progression.
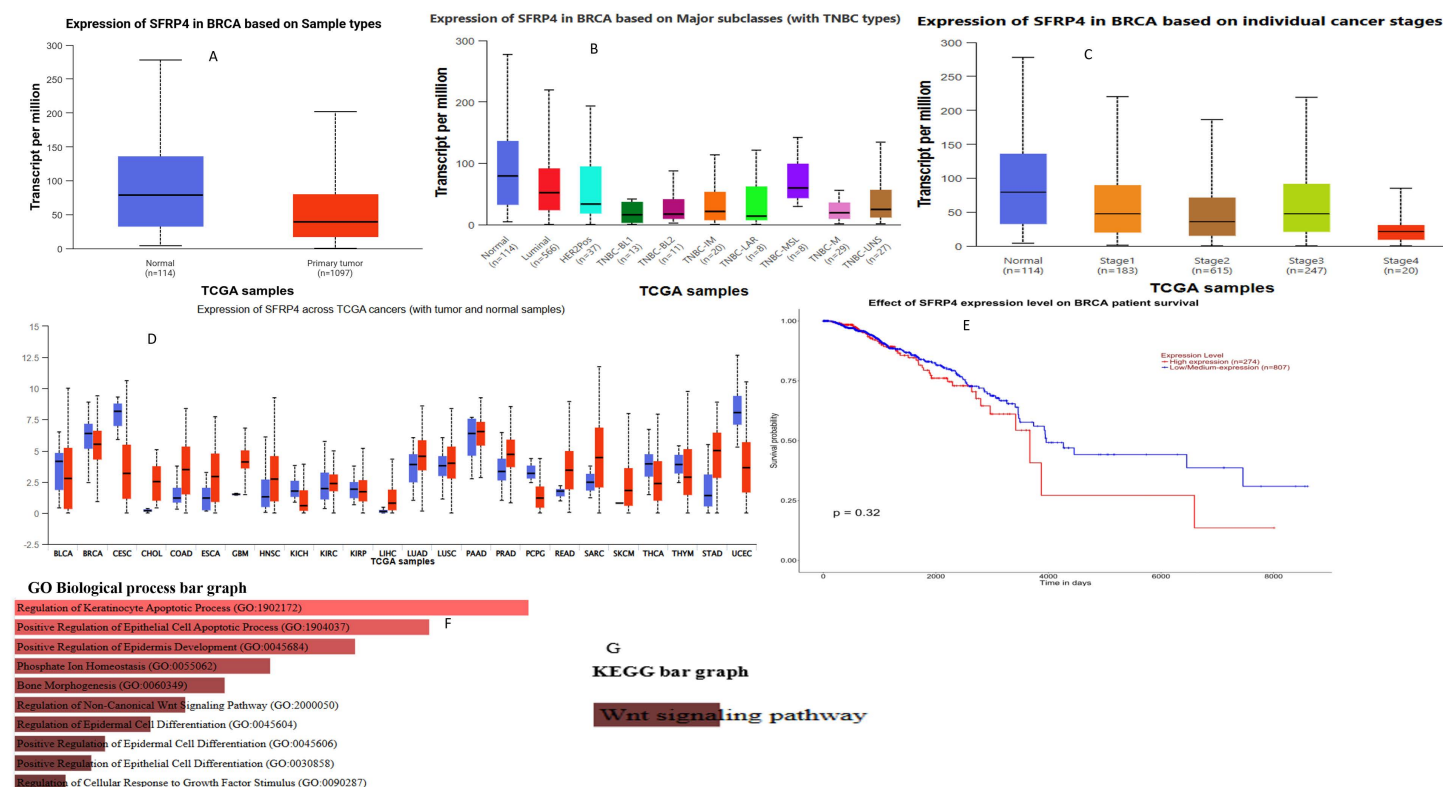

Fig 1. Expression of SFRP4 in A) Breast invasive carcinoma B) Main subtypes of breast cancer C) Individual D) with tumour and normal samples and, E) The Kaplan-Meier survival analysis and enrichment analysis of SFRP4 with, F) GO and G) KEGG biological process graph.

https://doi.org/10.1371/journal.pone.0331735.g001

Comparative analysis of *sFRP4* expression across various breast cancer subclasses revealed significantly higher levels in healthy volunteers compared to patients with TNBC and HER2 receptor-positive BC, as shown in Fig 1B. Fig 1C demonstrates that *sFRP4* expression is stable during the first three stages of breast cancer, followed by a significant decrease in stage 4. As shown in Fig 1E, Kaplan–Meier survival analysis did not reveal a statistically significant difference in overall survival between patients with high and low/medium sFRP4 expression levels (p = 0.32). Fig 1F and G show GO and KEGG biological processes, respectively. Although sFRP4 is typically downregulated in breast cancer and associated with tumor suppression through Wnt signaling inhibition, this finding suggests that its prognostic value in survival may be limited or influenced by tumor subtype, stage, or additional regulatory mechanisms [53–58]. To confirm the results obtained from the clinical cancer database, we examined the levels of *sFRP4* gene expression in MDA-MB-231 BC cell lines using ELISA and qPCR.

To determine which biochemical pathways were more abundant in this set of genes, the Enricher server was used, as shown in the picture. The gene set primarily governs non-canonical Wnt signaling and participates in the apoptotic process. An effective method for blocking the Wnt signalling pathways' beta-catenin compensation mechanism is to target *sFRP4* in breast cancer. In the analysis of TNBC cell lines, *sFRP4* expression was found to be slightly increased in MDA-MB-231, prompting the selection of this cell line for subsequent signalling investigations.

In-silico findings

Computational analyses such as molecular docking and ADMET profiling have produced favourable results. The complex underwent a 100-nanosecond molecular dynamics (MD) simulation in a water-based environment, and the resulting deviations, interaction graphs, and fluctuations were examined.

3D-structure modeling and validation

The structural analysis of the *sFRP4* was extensively performed in the study of Rehman et al. [21], focusing on its molecular composition, active sites, and stability. Active site residues, such as Glu60, Tyr61, Glu63, Leu64, and His117, were identified as critical for ligand interactions through *in-silico* docking, as in Fig 2.

Principal and molecular features of the ligand

Several potential therapeutic agents do not succeed in clinical trials because of their unsuitable ADMET properties. To evaluate the expected drug-likeness, ADME calculation is useful. Table 2 displays the aggregated ADMET endpoints. It
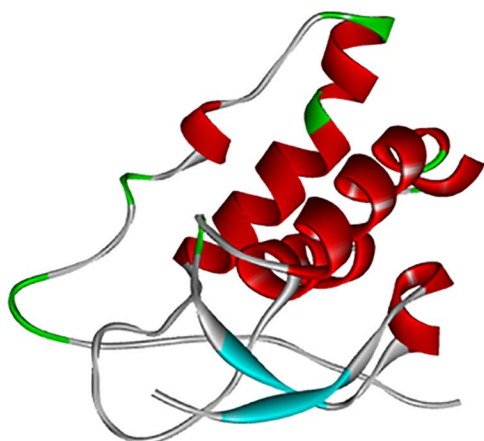

Fig 2. 3D structure of the SFRP4.

https://doi.org/10.1371/journal.pone.0331735.g002

Table 2. Evaluation of the two most effective drugs using the parameters supplied by the computational prediction approach for drug likeness.

Ligand	Parameter	Silibinin	Isotretinoin
Drug likeness	1. Molecular Weight (<500 Dalton) 2. (TPSA) (Å) 2 (<140) 3. Heavy atom count (n atoms) 4. H-bond donors (nOHNH) (≤5) 5. H-bond acceptors (nON) (≤10) 6. No. of rotatable bonds (≤10) 7. LogS 8. cLogP	482.12 155.1 4 35 5 10 4 −4.052 2.79	300.44 37.30 22 1 2 5 −3.905 4.186
Adsorption	1. Water solubility 2. Caco-2 Permeability 3. P glycoprotein inhibitor 4. Intestinal absorption (% absorbed) 5. Skin Permeability	−3.204 0.435 yes 61.861 −2.735	−4.924 1.61 No 94.419 −2.703
Distribution	1. BBB permeability (Log BB) 2. CNS permeability (Log PS)	No −3.639	0.236 −2.114
Metabolism	1. CYP2D6 Substrate 2. CYP3A4 Substrate 3. CYP1A2 Inhibitor C 4. YP2C19Inhibitor 5. CYP2C9 Inhibitor	No Yes NO No No	No Yes No Yes Yes
Excretion	1. Total Clearance (Log ml/min/kg) 2. Renal OCT2 substrate	−0.103 No	1.443 No
Toxicity	1. AMES toxicity 2. Skin Sensitization 3. Oral Rat Acute Toxicity (LD50) (mol/kg)	No No 2.559	No Yes 1.767

https://doi.org/10.1371/journal.pone.0331735.t002

is possible to deduce the molecular characteristics that are associated with drug-likeness by using five descriptors, which are as follows: the molecular weight (MW) must be ≤ 500 Da, the QPlogPo/w value must be five, the hydrogen acceptor must be ≤ 10, the hydrogen donor must be ≤ 10, and the Topological Polar Surface Area (TPSA) must be < 5. The standards follow the rule of five proposed by Lipinski. Most of the twenty-two parameters that make up the pharmacokinetic profile are within the acceptable range. The expected number of metabolic processes is within the permitted range, and the numbers are in line with the selected active ligand. The *sFRP4* protein molecular dynamics simulation and docked structures have been thoroughly examined for many factors. The chemical Silibinin and isotretinoin ADMET profile complies with Lipinski's rule of five, and the binding affinity.

The chosen ligands were all inert across the blood-brain barrier, had excellent intestinal solubility, and positive CaCO2 permeability. Having shown little inhibitory potential against CYP1A2 and CYP2C19, the ligands were also beneficial towards cytochrome P450 enzymes. All of the lead ligands had poor total and renal clearance. Lastly, the AMES toxicity test was successful for the lead ligands that were chosen based on their toxicity prediction findings. The lead ligand ADMET drug tests did, however, provide satisfactory findings, suggesting that these leads may be good candidates for treatment against sFRP4.

Protein-ligand interaction analysis

Of the 100 bioactive compounds analysed, merely three compounds (Silibinin, Isotretinoin, and Aristolochic acid) displayed binding energies lower than −6 kcal/mol, as shown in Table 3.

Among the three compounds analysed, only Silibinin demonstrated binding affinity to the designated receptor binding site, establishing robust polar interactions with three critical residues, specifically Glu63 and Gln60. Furthermore, it was

Table 3. Molecular docking energy values of SFRP4 with candidate compounds.

Sr. No	Ligand Name	Molecular Formula	Binding Score (Kcal/mol)	Interacting Residues in the Active Pocket
1	Silibinin	C25H22O10	−7.5	Met112,Pro120,Leu64, Glu63 and Gln60
2	Isotretoinin	C20H28O2	−6.2	Val67,Tyr115,Leu64, His 117,Met112, Tyr61
3	Aristolochic acid(2236)	C17H11NO7	−6	Gln60,Pro120,Ty61Met112
4	Isorhamnetin	C16H12O7	−5.9	Leu64,Tyr61,Pro120
5	Lupeol	C30H50O	−5.9	Tyr61,Leu64,His117,Pro120,His48,Met112
6	Stigmasterol	C29H48O	−5.8	Tyr61,Pro120,Met112,Leu64
7	Caffeic Acid	C9H8O4	−5.5	His117,Glu63
8	Isoeugenol	C10H12O2	−5	Met112,Leu64

https://doi.org/10.1371/journal.pone.0331735.t003

demonstrated that Silibinin established highly stable interactions with critical residues, specifically Glu63 and Gln60 within the hydrophobic cleft of the target site as in Fig 3A, whereas the ligand isotretinoin exhibited three types of interfaces Pi-Pi stacking, Pi-sigma, and Pi-alkyl with amino acids Tyr61, Tyr115, His117, Val, Met112, and Leu64 on the target protein as shown in Fig 3B.

Modelling the protein-ligand interaction

The docked structure underwent simulation for a duration of 100 ns following the equilibration phase, during which multiple metrics were plotted to demonstrate its stability. Trajectories were extensively analysed, with RMSD, RMSF, and intermolecular interactions identified throughout the simulation.

Root mean square deviation and root mean square fluctuations

RMSD is utilized to quantify exact deviations throughout the simulation time, and our research investigated their entire courses. Fig 4A, A′ illustrates the RMSD for Silibinin complex, and Fig 4B, B′ indicates the isotretinoin complex, and the secreted protein *sFRP4*, which is the target protein, ranges from 0 to 100 nanoseconds.

The protein in the Silibinin protein complex exhibited an initial variation of 2.5 Å, and the ligand a deviation of 16 Å between 0 and 10 nanoseconds.

Fig 4A illustrates the dynamic stability of both the protein (Cα atoms) and the ligand over a 100-nanosecond molecular dynamics simulation. The protein RMSD (blue line) shows an initial rise during the first 10 ns, stabilizing around 2.8–3.0
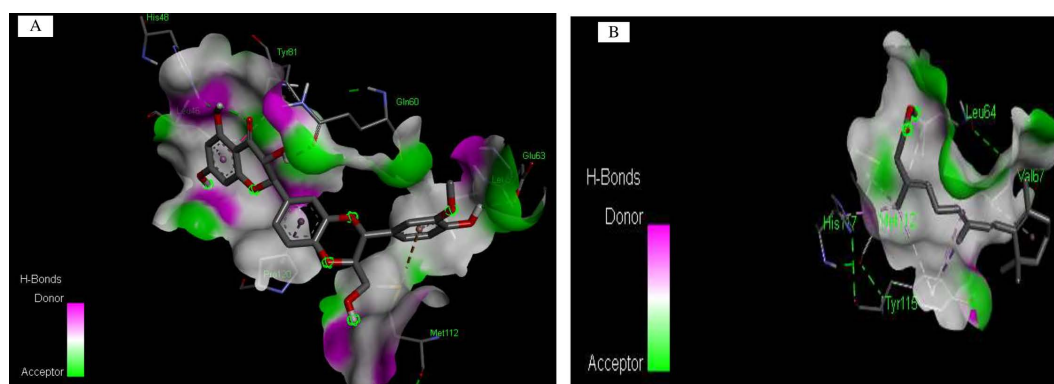

Fig 3. Predicted binding conformation of Silibinin and Isotretinoin with the designated ligand-binding site of sFRP4. A, B Interfaces are produced through the participation of protein-ligand complexes.
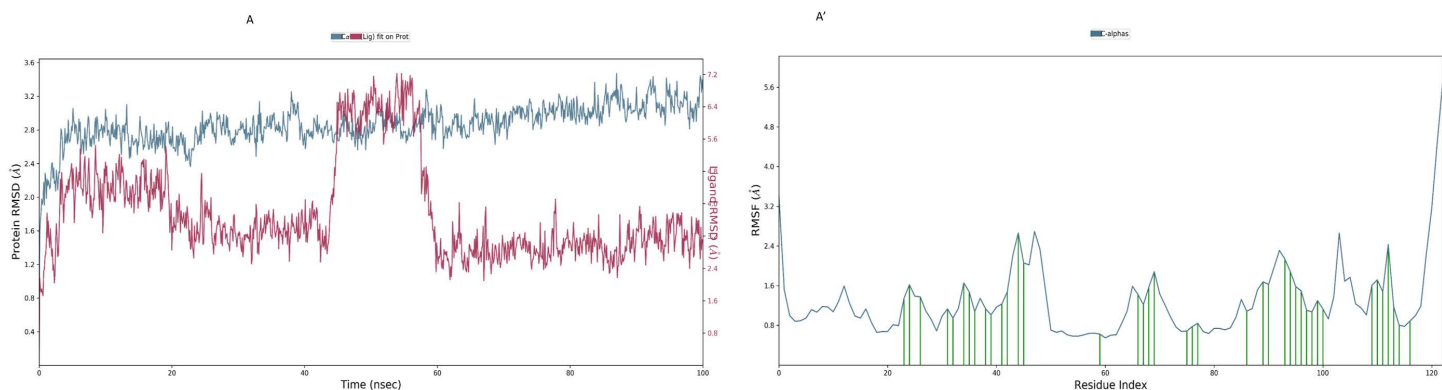
https://doi.org/10.1371/journal.pone.0331735.g003

Fig 4. MD. Simulation results in A, A′: Protein RMSD and RMSF for Silibinin complex.

Å for the remainder of the simulation, indicating that the protein maintains a relatively stable conformation throughout. In contrast, the ligand RMSD (maroon line) exhibits more fluctuation. Initially, the ligand RMSD increases and fluctuates between 2.0–3.0 Å up to around 45 ns, suggesting moderate conformational flexibility within the binding pocket. However, a sharp spike is observed between approximately 45–58 ns, reaching up to ~7.2 Å, which may indicate a significant conformational change or partial unbinding event. After this spike, the ligand RMSD drops and stabilizes around 3.0 Å, suggesting that the ligand rebinds or adopts a new stable conformation. Overall, while the protein remains structurally stable, the ligand undergoes transient instability, possibly reflecting flexible binding dynamics or alternate binding modes within the active site. This conformational event was consistently observed across all three replicate simulations, confirming it is a genuine feature of the ligand's dynamics rather than a simulation artifact.

Based on the RMSF analysis of Silibinin complex Fig 4A′ shown in the graph, most of the Cα residues display fluctuations below 3.0 Å, indicating that the protein maintains overall structural stability throughout the simulation. However, elevated flexibility is observed at specific regions, particularly near the C-terminal end (e.g., around residue 120), where the RMSF reaches approximately 5.6 Å. This localized mobility may reflect solvent-exposed loops or terminal regions with dynamic roles in the protein's function. Notably, residues such as GLN60 and GLU63 exhibit moderate fluctuations yet are critical in maintaining the stability of the protein-ligand complex, as they are involved in hydrogen bonding interactions with the ligand. Additionally, hydrophobic contacts between the ligand and residues Met112, Pro120, and Leu64 suggest key stabilizing interactions at the binding interface. These findings underscore the functional importance of these residues in ligand recognition and binding, highlighting them as potential targets in structure-based drug design. The combination of stable core residues and flexible interaction regions provides valuable insight into the dynamic behaviour of the protein during molecular recognition events.

Fig 5B shows the RMSD values for both the protein and the ligand over a 100 ns period. Initially, at 0 ns, both RMSD values are low, indicating stability in both structures. As the simulation progresses, the protein experiences larger fluctuations in RMSD, but the values remain below 3 Å, suggesting it maintains its overall structure with only minor conformational changes. The ligand's RMSD fluctuates less and stays under 3 Å throughout, indicating that it remains in a stable conformation within the protein's binding site. Both structures stabilize around 90–100 ns, with minimal deviation. The protein's RMSD values are slightly higher, showing more flexibility, while the ligand's lower RMSD signifies its stable binding.

Our analysis of the Cα and ligand contacts for the RMSF in Fig 5B′ revealed that the ligand isotretinoin interacts hydrophobically with Met112 and Leu64. Hydrophobic contacts are generated at Tyr61, Tyr115, His117, Val, Met112, and Leu64 amino acids (active site) on the protein by the ligand isotretinoin. Overall, most of the protein remains stable with RMSF
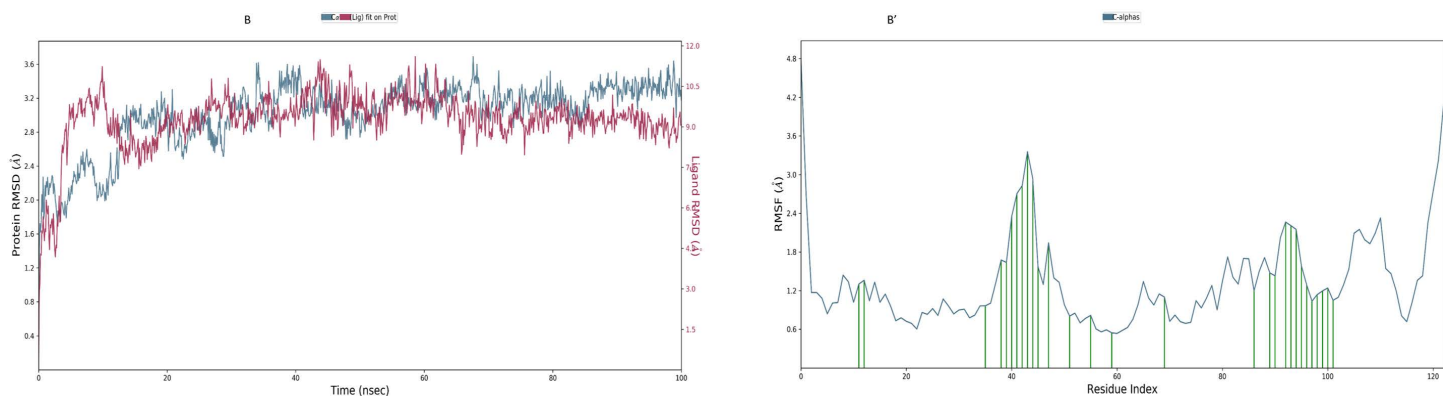
Fig 5. MD. Simulation results in (B, B′): Protein RMSD and RMSF for Isotretinoin complex.

values below 3.0 Å, indicating secure structural integrity during the simulation. The localized flexibility in specific regions may contribute to the protein's dynamic behaviour or interactions, making these areas of interest for further investigation.

Simulation interaction analysis

Stable receptor-ligand interactions rely on the interaction strengths between the ligand and the target protein, *sFRP4*, making it essential to identify the amino acid residues that engage with the ligands via molecular dynamics simulations. Fig 6A, A′ highlights that Silibinin interacts with its protein target through a combination of hydrogen bonding, hydrophobic interactions, and water-mediated bridges, primarily involving residues GLN60, GLU63, LEU46, PRO120, and MET112. These interactions contribute significantly to the stability and binding affinity of the Silibinin protein complex during molecular dynamics simulations.

Fig 7B, B′ shows that the ligand primarily interacts with the protein through hydrophobic interactions (e.g., with MET112, TYR115, VAL67, and LEU46) and is stabilized by water-mediated bridges. The interaction diagram shows 2D interaction maps of docked complexes based on bioactive compounds, which illustrate how interactions are preserved over the simulation trajectory. Compounds Silibinin and Isotretinoin were similar to the co-crystal ligand's acceptor and donor hydrogen bond characteristics. Significant interactions between Silibinin's hydrogen bonds were highlighted by the counts of donor and acceptor bonds. The compounds Silibinin and Isotretinoin were shown in 2D interaction maps as having hydrogen bonds, pi-pi T-shaped, alkyl interactions, pi-sigma interactions, and pi-alkyl interactions, respectively.

These interactions illustrate how high-energy aromatic amino acid constituents are expected to be involved in organizing the adenine ring within the protein during its production. In addition, electrostatic interactions were observed between the various components of the amino acid composition. Figs 6 and 7 illustrate the quantity of unique intermolecular interactions established by all pocket residues with the ligand-binding area. The compounds isotretinoin and Silibinin were successfully docked and verified for higher-quality docking outcomes. Certain residues showed comparable hydrophobic and hydrogen bonding properties to those of amino acids.

In-vitro study

Anti-proliferative activity in MDA-MB-231 (TNBC) cell. Silibinin and Isotretinoin, identified as promising compound candidates through in silico results, were tested for their toxicity on MDA-MB-231 (TNBC) cells using the MTT method. As shown in Fig 8, Silibinin and Isotretinoin reduced the cell viability in a time- and dose-dependent manner. The results suggest that both compounds were not toxic for normal cells, showing their specific toxicity against the breast cancer cell line. Hence, Silibinin and Isotretinoin suppress cell growth and proliferation of MDA-MB-231 cells.
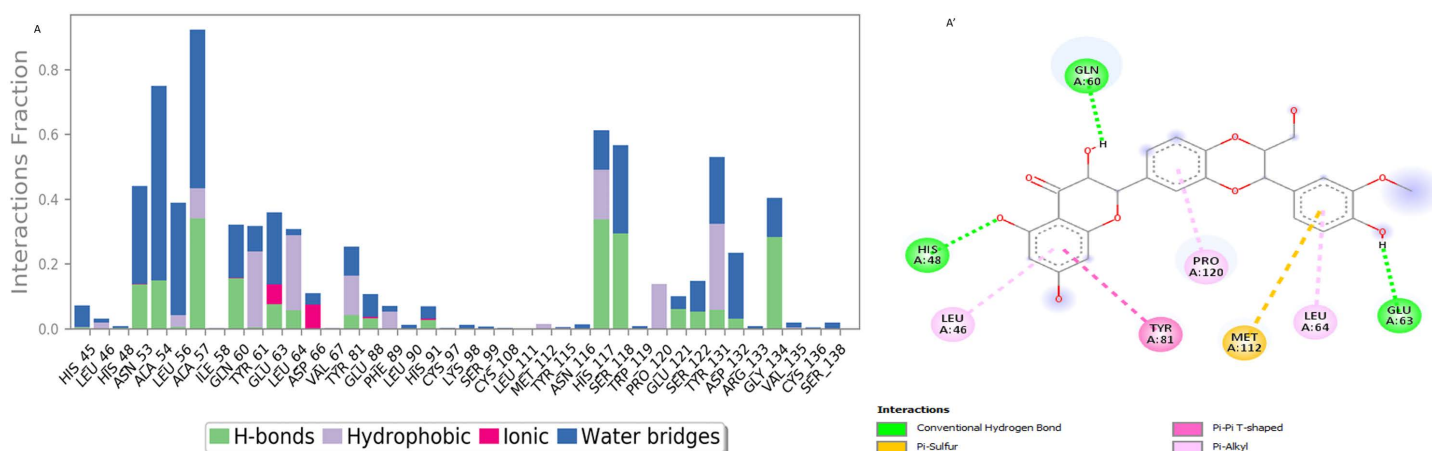
Fig 6. Simulation interaction diagram of silibinin (A, A′) 2-D interactions illustration of the protein–Ligand.
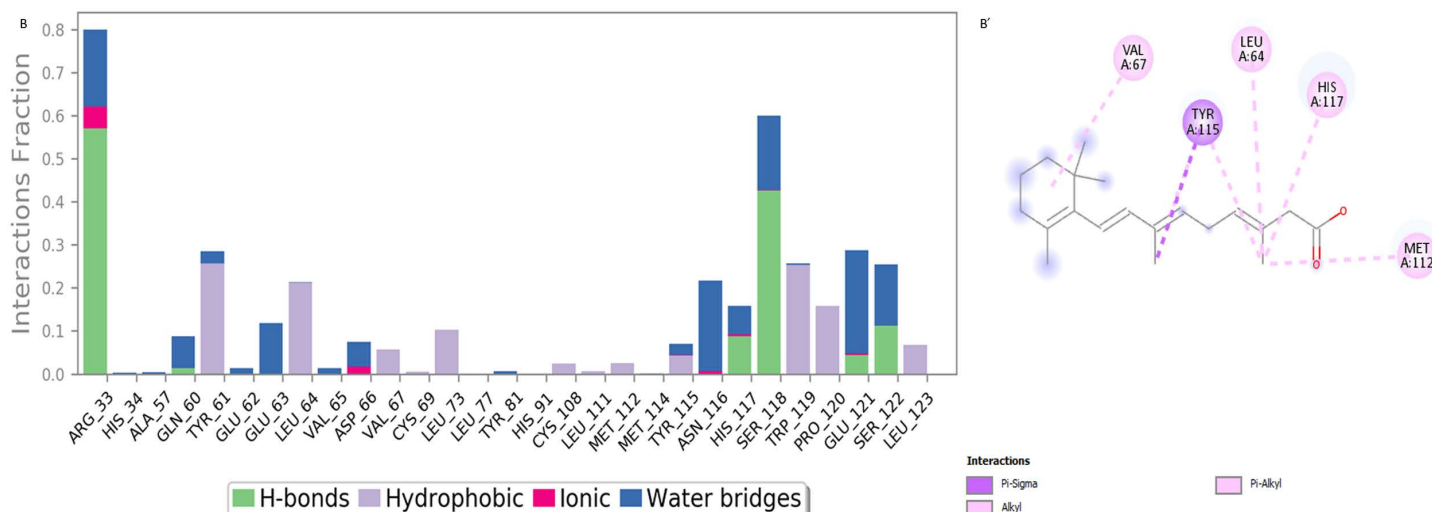
https://doi.org/10.1371/journal.pone.0331735.g006

Fig 7. Simulation interaction diagram of isotretinoin (B, B′) 2-D interactions illustration of the protein–Ligand.

https://doi.org/10.1371/journal.pone.0331735.g007

Silibinin and isotretinoin inhibit the migration of MDA-MB-231 cells

Since Silibinin has previously demonstrated the ability to suppress invasion in different cancer cell lines with other targets [59–62]. Previous studies have demonstrated that 13CRA (isotretinoin) can impede the multiplication of cancer cells, namely those associated with the stomach and breast [63]. We tested whether Silibinin and Isotretinoin could also exert anti-metastatic effects in breast cancer cells. This experiment used an in vitro wound healing test to estimate the Silibinin effects and Isotretinoin on migrating MDA-MB-231 cells. The number of cells that migrated into the scratched region was determined by taking pictures after treatment began, and then the percentage of migration was calculated from those numbers. Fig 9A and B illustrates the outcomes of the migratory capacity assessment conducted on MDA-MB-231 cells by a wound-healing assay.
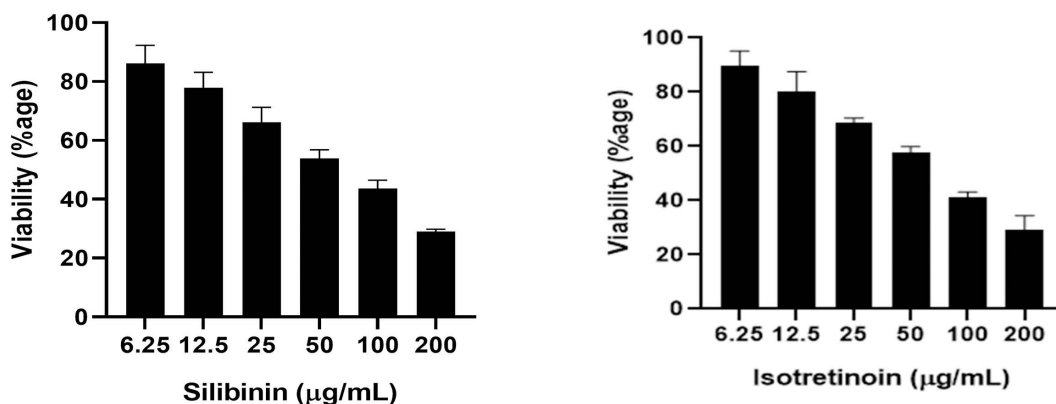
Fig 8. Anti-proliferative activity of Silibinin and isotretinoin in a dose-dependent manner by MTT assay.

https://doi.org/10.1371/journal.pone.0331735.g008

According to Fig 9A, B, during a 24-hour incubation period for injured cells, the groups treated with Silibinin and Isotretinoin showed an increase in percentage wound width at 12, 25, and 50 µg/ml, respectively. According to the study's findings, it considerably and independently decreased the migration of triple-negative breast cancer cells MDA-MB-231.

Expression analysis of *sFRP4*

Based on the ELISA results, both compounds exhibited remarkable inhibition of cell proliferation by blocking the binding of Wnt protein in the Wnt signalling pathway, and *sFRP4* expression was upregulated. In contrast, beta-catenin signalling overactivation significantly reduced *sFRP4* expression in breast cancer cells Fig 10A, B. Cells were harvested in order to use ELISA to measure the expression levels of *sFRP4*.

Quantitative real-time polymerase chain reaction (qPCR)

Real-time qPCR was employed to evaluate the influence of both medications on the expression of Wnt/β-catenin target genes, namely the *sFRP4* tumour suppressor gene, following 24 hours of exposure to MDA-MB-231. A notable downregulation of Wnt gene expression and an upregulation of the *sFRP4* tumour suppressor gene were detected in a dose-dependent manner in Fig 10C.

Discussion

Breast cancer development, metastatic dispersion, stemness, and resistance to multiple drugs have been linked to a complicated interaction of numerous signalling pathways that restrict the patient's overall survival and effective treatment targeting [64]. Bioinformatics analysis revealed that *sFRP4* is a viable target for TNBC treatment. Gene expression research indicated aberrant *sFRP4* expression in a diversity of malignancies, including breast cancer. The possible functions of the main signalling pathways involving *sFRP4* in cancer development were further highlighted by the pathway enrichment analysis. Furthermore, docking investigations of *sFRP4* with various drugs and inhibitors have shown that Silibinin and Isotretinoin have the highest binding energy, making it the most promising choice.

The binding energies of the repurposed drugs isotretinoin and Silibinin with *sFRP4* were greater than those of the other compounds. It is necessary to recognize the intrinsic drawbacks of molecular docking, including its dependence on static structures and the possibility of inaccurate predictions of dynamic protein-ligand interactions. To overcome these limitations and improve the stability of the results, molecular dynamics (MD) simulations were used. These further investigations confirmed the potential effectiveness of Silibinin and Isotretinoin in contrast to the control inhibitors by shedding light
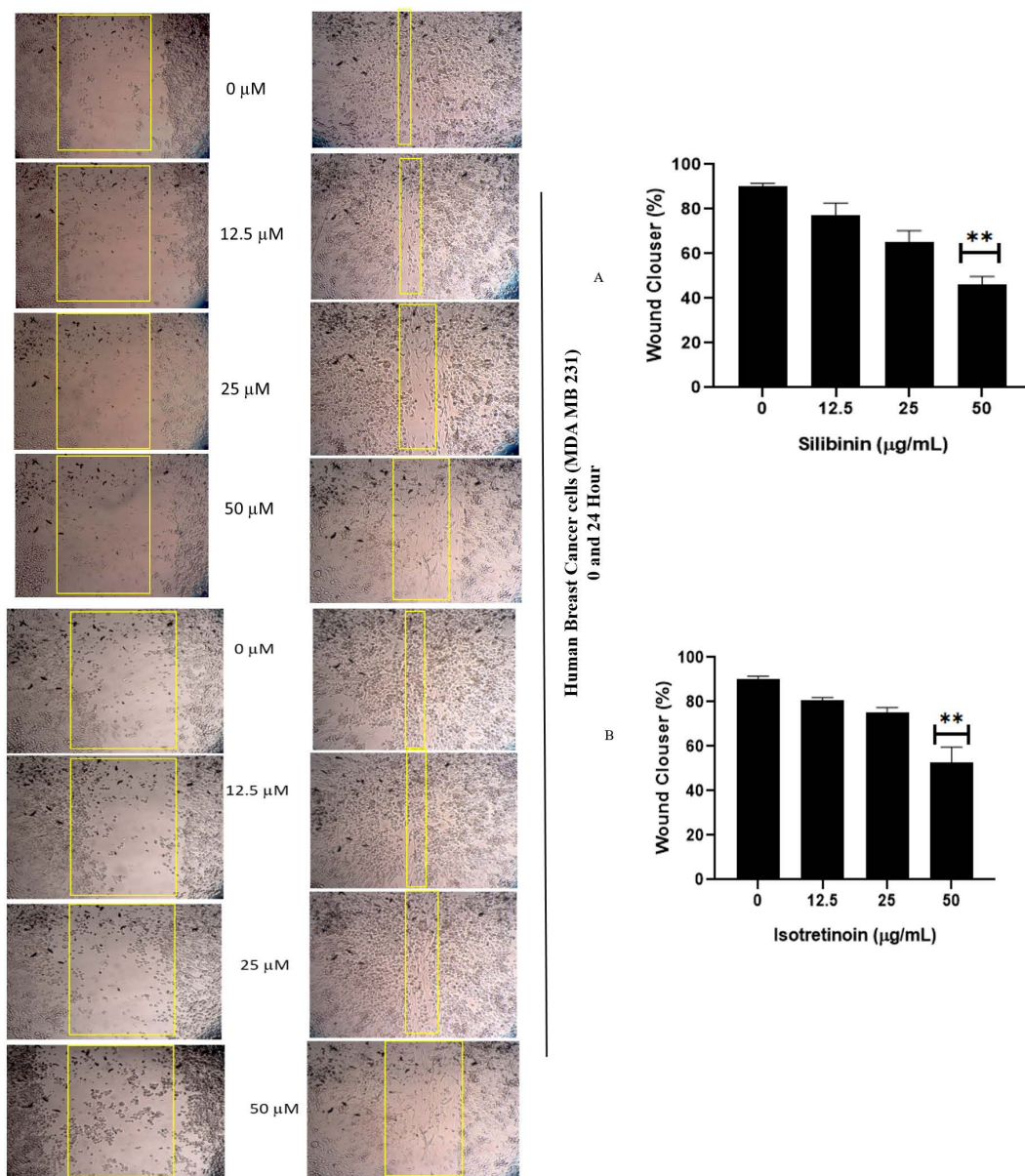
Fig 9. Silibinin and isotretinoin (A, B) stop MDA-MB-231 cells from migrating. Means ± SD of three separate experiments provide the data reported in A and B. **P < 0.01 in comparison to the control cohort.

on their binding stability with the target proteins. According to the findings of the MD simulation, Silibinin had a stronger and more consistent interaction with *sFRP4*. It is shown that Silibinin has stronger electrostatic and van der Waals forces. It was stated that Silibinin and Isotretinoin had a robust interaction with the target proteins.

In-vitro experiments were used to confirm the in-silico predictions of Silibinin and Isotretinoin's anticancer therapeutic potential. Cell lines MDA MB 231 were chosen for the in vitro investigation due to their resemblance to human-origin breast cancer [65]. With the tetrazolium-based MTT assay, the cytotoxic effects of isotretinoin and Silibinin on these cells were evaluated [66]. Previous studies indicate that compounds at elevated concentrations (150–250 µM) inhibit cell
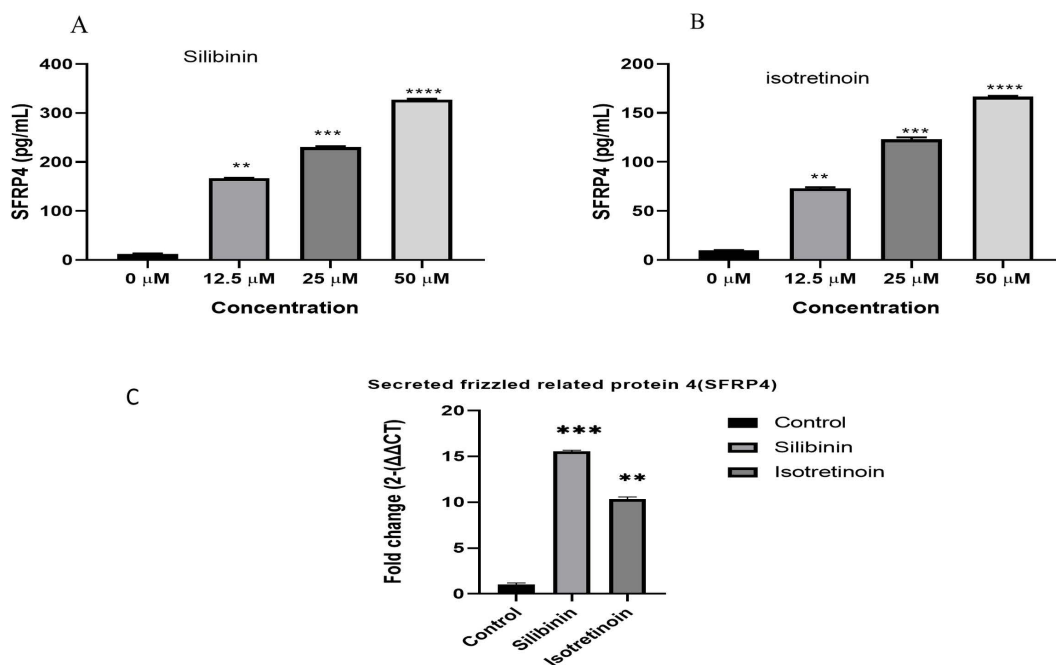
Fig 10. The expression of sFRP4 in TNBC MDA-MB-231 cell lines after treatment with silibinin and isotretinoin and its subsequent effects. The cells were subjected to a range of doses of silibinin and isotretinoin, ranging from 12.5 to 50 μM, for 48 hours. The findings of these investigations are presented as the means ± standard error of the mean (SEM) from three separate experiments. Statistical significance was assessed in Figures A and B. Effect of Silibinin and Isotretinoin affects the mRNA expression of the Wnt/β-catenin antagonist sFRP4 following 48 hours of exposure. Comparatively to untreated controls, both compounds affect the expression of sFRP4 gene in Figure C (**$P < 0.05$, ***$P < 0.001$).

proliferation, leading to apoptosis in MDA-MB-231 cells [67,68]. The results demonstrate that the MDA-MB-231 cells' ability to migrate and invade is inhibited at lower doses of the two bioactive compounds. These findings were determined to be consistent with other studies [63,67,69,70]. Silibinin and Isotretinoin were shown to have anticancer properties in vitro. Interestingly, in EMT-induced TNBC cells, the IC50 for both drugs was decreased. Isotretinoin and Silibinin increased oxidative stress and ROS production, and upregulated the Wnt antagonist sFRP4, according to the results.

Through the production of ROS, both potent hits mechanistically cause TNBC cells to undergo apoptosis, which results in cell death [69]. Furthermore, prior research has demonstrated that the activation of the Wnt/β-catenin signaling pathway occurs more often in TNBC and is associated with worse clinical outcomes [71,72]. The case for sFRP4 as a breast cancer therapeutic target is becoming stronger by the day. Several investigations have shown that Silibinin has cytotoxic effects on breast cancer cells: these effects were shown [73–75].

To further our comprehension of how retinoids impede the progression of breast cancer cell lines, we investigated the effect of 13cRA on inducing apoptosis in the MDA-MB-231 cell line of breast cancer. Proliferation experiments provide dose-dependent evidence that 13cRA (isotretinoin) inhibits cell growth in MDA-MB-231 cell lines. Furthermore, we found that Silibinin can upregulate the expression of the sFRP4 gene and suppress the Wnt/β-catenin signaling pathway in breast cancer cells. Furthermore, we discovered that the effects of Silibinin on the Wnt/β-catenin signalling pathway occurred at doses that were equivalent to those necessary to reduce the proliferation of breast cancer cells. Taken together these data indicate that 13-cis RA inhibit the cell growth and induces apoptosis in breast cancer cell line by a RAR-independent mechanism. The inhibitory effects of both drugs on MDA-MB-231 are associated with its anti-breast cancer properties.

Breast cancer cells (TNBC) are distinguished by their increased Wnt/beta-catenin activity, which promotes cell migration and results in an invasive phenotype. The overexpression of downstream genes, including Cyclin D1 and CD44, has been associated with the disruption of the Wnt/β-catenin signaling cascade [76–78]. The investigation of gene expression by RT-PCR shown that both drugs markedly suppressed the expression of genes associated with the beta-catenin cascade. Furthermore, both Silibinin and Isotretinoin were shown to significantly (P < 0.05) enhance the expression of the tumour suppressor gene *sFRP4*. Ultimately, the discovery of this signalling network that drives EMT development in TNBC paves the way for novel treatment approaches that precisely target the gene which is part of this signalling cascade.

Conclusion

This investigation established Silibinin and Isotretinoin as promising therapeutic agents that effectively upregulate the Wnt antagonist *sFRP4* in TNBC. Molecular docking and dynamic simulations confirmed strong, stable interactions with *sFRP4*, particularly for Silibinin. In vitro assays revealed dose-dependent cytotoxicity, reduced migration, and significant upregulation of *sFRP4*, leading to apoptosis in MDA-MB-231 cells. These findings position *sFRP4* as a promising therapeutic target for TNBC. In-vivo pharmacodynamics and safety characteristics of these molecules should be investigated in further studies. Investigating combination therapies with other pathway inhibitors could enhance anticancer efficacy. Long-term studies on resistance mechanisms and bioavailability will further refine their clinical applicability.

Supporting information

S1 File.
(DOCX)

Author contributions

Conceptualization: Rehana Ramzan, Shazia Anwer Bukhari, Azhar Rasul.

Data curation: Rehana Ramzan, Shazia Anwer Bukhari, Azhar Rasul.

Formal analysis: Rehana Ramzan, Shazia Anwer Bukhari, Azhar Rasul.

Investigation: Shazia Anwer Bukhari.

Methodology: Rehana Ramzan, Shazia Anwer Bukhari, Azhar Rasul.

Project administration: Shazia Anwer Bukhari.

Resources: Shazia Anwer Bukhari.

Software: Shazia Anwer Bukhari.

Supervision: Rehana Ramzan, Shazia Anwer Bukhari, Azhar Rasul.

Validation: Shazia Anwer Bukhari, Azhar Rasul.

Writing – original draft: Rehana Ramzan, Azhar Rasul.

Writing – review & editing: Rehana Ramzan, Shazia Anwer Bukhari, Azhar Rasul.

References

1. Hussein M, Elnahas M, Keshk A. A framework for predicting breast cancer recurrence. Expert Systems with Applications. 2024;240:122641.
2. Kizhakkeppurath Kumaran A, Sahu A, Singh A, Aynikkattil Ravindran N, Sekhar Chatterjee N, Mathew S, et al. Proteoglycans in breast cancer, identification and characterization by LC-MS/MS assisted proteomics approach: A review. Proteomics Clin Appl. 2023;17(4):e2200046. https://doi.org/10.1002/prca.202200046 PMID: 36598116
3. Daniele A, Divella R, Pilato B, Tommasi S, Pasanisi P, Patruno M, et al. Can harmful lifestyle, obesity and weight changes increase the risk of breast cancer in BRCA 1 and BRCA 2 mutation carriers? A Mini review. Hered Cancer Clin Pract. 2021;19(1):45. https://doi.org/10.1186/s13053-021-00199-6 PMID: 34706754

4. Obeagu EI, Obeagu GU. Breast cancer: A review of risk factors and diagnosis. Medicine (Baltimore). 2024;103(3):e36905. https://doi.org/10.1097/MD.0000000000036905 PMID: 38241592

5. Sund M, Garmo H, Andersson A, Margolin S, Ahlgren J, Valachis A. Estrogen therapy after breast cancer diagnosis and breast cancer mortality risk. Breast Cancer Res Treat. 2023;198(2):361–8. https://doi.org/10.1007/s10549-023-06871-w PMID: 36773184

6. Sahu A, Pradhan D, Veer B, Kumar S, Singh R, Raza K, et al. In silico screening, synthesis, characterization and biological evaluation of novel anticancer agents as potential COX-2 inhibitors. Daru. 2023;31(2):119–33. https://doi.org/10.1007/s40199-023-00467-x PMID: 37454036

7. Sahu A, Verma S, Varma M, Yadav MK. Impact of ErbB receptors and anticancer drugs against breast cancer: a review. Current Pharmaceutical Biotechnology. 2022;23(6):787–802.

8. Bukhari SA, Shamshari WA, Ur-Rahman M, Zia-Ul-Haq M, Jaafar HZE. Computer aided screening of secreted frizzled-related protein 4 (SFRP4): a potential control for diabetes mellitus. Molecules. 2014;19(7):10129–36. https://doi.org/10.3390/molecules190710129 PMID: 25019556

9. Arora A, Scholar EM. Role of tyrosine kinase inhibitors in cancer therapy. J Pharmacol Exp Ther. 2005;315(3):971–9. https://doi.org/10.1124/jpet.105.084145 PMID: 16002463

10. Yadav MK, Sahu A, Anu Kasturria N, Priyadarshini A, Gupta A. Clinical applications of protein-based therapeutics. Protein-Based Therapeutics. Springer; 2023. p. 23–47.

11. Pohl S, Scott R, Arfuso F, Perumal V, Dharmarajan A. Secreted frizzled-related protein 4 and its implications in cancer and apoptosis. Tumor Biology. 2015;36:143–52.

12. Bovolenta P, Esteve P, Ruiz JM, Cisneros E, Lopez-Rios J. Beyond Wnt inhibition: new functions of secreted Frizzled-related proteins in development and disease. J Cell Sci. 2008;121(Pt 6):737–46. https://doi.org/10.1242/jcs.026096 PMID: 18322270

13. Pawar NM, Rao P. Secreted frizzled related protein 4 (sFRP4) update: A brief review. Cell Signal. 2018;45:63–70. https://doi.org/10.1016/j.cellsig.2018.01.019 PMID: 29360572

14. Müller D, Győrffy B. DNA methylation-based diagnostic, prognostic, and predictive biomarkers in colorectal cancer. Biochim Biophys Acta Rev Cancer. 2022;1877(3):188722. https://doi.org/10.1016/j.bbcan.2022.188722 PMID: 35307512

15. Ramazi S, Dadzadi M, Sahafnejad Z, Allahverdi A. Epigenetic regulation in lung cancer. MedComm (2020). 2023;4(6):e401. https://doi.org/10.1002/mco2.401 PMID: 37901797

16. Ma Z, Zang W, Wang H, Wei X. Silibinin enhances anti-renal fibrosis effect of MK-521 via downregulation of TGF-β signaling pathway. Human Cell. 2020;33.

17. Sharma A, Kumar S, Pahil V, Mamoria B, Yadav M, Sehrawat N, et al. Anticancer therapeutic potential of silibinin: current trends, scope and relevance. Med Chem Res. 2025;34(4):809–24. https://doi.org/10.1007/s00044-025-03383-8

18. Cava C, Castiglioni I. Integration of molecular docking and in vitro studies: A powerful approach for drug discovery in breast cancer. Appl Sci. 2020;10(19):6981.

19. Davies M, Nowotka M, Papadatos G, Dedman N, Gaulton A, Atkinson F, et al. ChEMBL web services: streamlining access to drug discovery data and utilities. Nucleic Acids Res. 2015;43(W1):W612-20. https://doi.org/10.1093/nar/gkv352 PMID: 25883136

20. Paul SM, Mytelka DS, Dunwiddie CT, Persinger CC, Munos BH, Lindborg SR, et al. How to improve R&D productivity: the pharmaceutical industry's grand challenge. Nat Rev Drug Discov. 2010;9(3):203–14. https://doi.org/10.1038/nrd3078 PMID: 20168317

21. Rehman A, Bukhari SA, Akhter N, Ijaz Hussain MA, Chauhdary Z. In Silico identification of novel phytochemicals that target SFRP4: An early biomarker of diabesity. PLoS One. 2023;18(11):e0292155. https://doi.org/10.1371/journal.pone.0292155 PMID: 37943820

22. Waterhouse A, Bertoni M, Bienert S, Studer G, Tauriello G, Gumienny R, et al. SWISS-MODEL: homology modelling of protein structures and complexes. Nucleic Acids Res. 2018;46(W1):W296–303. https://doi.org/10.1093/nar/gky427 PMID: 29788355

23. Wiederstein M, Sippl MJ. ProSA-web: interactive web service for the recognition of errors in three-dimensional structures of proteins. Nucleic Acids Res. 2007;35(Web Server issue):W407-10. https://doi.org/10.1093/nar/gkm290 PMID: 17517781

24. Laskowski RA, MacArthur MW, Moss DS, Thornton JM. PROCHECK: a program to check the stereochemical quality of protein structures. Applied Crystallography. 1993;26(2):283–91.

25. Colovos C, Yeates TO. Verification of protein structures: patterns of nonbonded atomic interactions. Protein science. 1993;2(9):1511–9.

26. A Y, Bukhari SA, Zahoor MK, Mustafa G, Rasul A. Screening of novel phytochemicals as secreted frizzled-related protein 4 inhibitors: an early stage biomarker of type 2 diabetes. Pakistan Journal of Pharmaceutical Sciences. 2020;33(3):1245–50.

27. Kim S, Chen J, Cheng T, Gindulyte A, He J, He S, et al. PubChem 2025 update. Nucleic Acids Res. 2025;53(D1):D1516–25. https://doi.org/10.1093/nar/gkae1059 PMID: 39558165

28. Vélez-Vargas LC, Santa-González GA, Uribe D, Henao-Castañeda IC, Pedroza-Díaz J. In Vitro and In Silico Study on the Impact of Chlorogenic Acid in Colorectal Cancer Cells: Proliferation, Apoptosis, and Interaction with β-Catenin and LRP6. Pharmaceuticals (Basel). 2023;16(2):276. https://doi.org/10.3390/ph16020276 PMID: 37259421

29. Nguyen Thi Thu H, Nguyen Huu Huong D, Nguyen Thi Dieu T, Tran Thi Ngoc H, Pham Van H, Hoang Thi Ngoc A, et al. In vitro and in silico cytotoxic activities of triterpenoids from the leaves of Aralia dasyphylla Miq. and the assessment of their ADMET properties. J Biomol Struct Dyn. 2023;41(12):5863–71. https://doi.org/10.1080/07391102.2022.2098822 PMID: 35838156

30. Chen J, Wang J, Yang W, Zhao L, Hu G. Conformations of KRAS4B Affected by Its Partner Binding and G12C Mutation: Insights from GaMD Trajectory-Image Transformation-Based Deep Learning. J Chem Inf Model. 2024;64(17):6880–98. https://doi.org/10.1021/acs.jcim.4c01174 PMID: 39197061

31. Lipinski CA. Rule of five in 2015 and beyond: Target and ligand structural limitations, ligand chemistry structure and drug discovery project decisions. Adv Drug Deliv Rev. 2016;101:34–41. https://doi.org/10.1016/j.addr.2016.04.029 PMID: 27154268

32. Lipinski CA. Drug-like properties and the causes of poor solubility and poor permeability. J Pharmacol Toxicol Methods. 2000;44(1):235–49. https://doi.org/10.1016/s1056-8719(00)00107-6 PMID: 11274893

33. Daina A, Michielin O, Zoete V. SwissADME: a free web tool to evaluate pharmacokinetics, drug-likeness and medicinal chemistry friendliness of small molecules. Sci Rep. 2017;7:42717. https://doi.org/10.1038/srep42717 PMID: 28256516

34. Xiong G, Wu Z, Yi J, Fu L, Yang Z, Hsieh C, et al. ADMETlab 2.0: an integrated online platform for accurate and comprehensive predictions of ADMET properties. Nucleic Acids Res. 2021;49(W1):W5–14. https://doi.org/10.1093/nar/gkab255 PMID: 33893803

35. Banerjee P, Eckert AO, Schrey AK, Preissner R. ProTox-II: a webserver for the prediction of toxicity of chemicals. Nucleic Acids Res. 2018;46(W1):W257–63. https://doi.org/10.1093/nar/gky318 PMID: 29718510

36. Pires DE, Blundell TL, Ascher DB. pkCSM: predicting small-molecule pharmacokinetic and toxicity properties using graph-based signatures. Journal of medicinal chemistry. 2015;58(9):4066–72.

37. Azzam KA. SwissADME and pkCSM webservers predictors: An integrated online platform for accurate and comprehensive predictions for in silico ADME/T properties of artemisinin and its derivatives. Kompleksnoe Ispolzovanie Mineralnogo Syra= Complex use of mineral resources. 2023;325(2):14–21.

38. Gu Y, Yu Z, Wang Y, Chen L, Lou C, Yang C, et al. admetSAR3.0: a comprehensive platform for exploration, prediction and optimization of chemical ADMET properties. Nucleic Acids Res. 2024;52(W1):W432–8. https://doi.org/10.1093/nar/gkae298 PMID: 38647076

39. Graef J, Ehrt C, Rarey M. Binding Site Detection Remastered: Enabling Fast, Robust, and Reliable Binding Site Detection and Descriptor Calculation with DoGSite3. J Chem Inf Model. 2023;63(10):3128–37. https://doi.org/10.1021/acs.jcim.3c00336 PMID: 37130052

40. Hassan M, Azhar M, Abbas Q, Raza H, Moustafa AA, Shahzadi S, et al. Finding Novel Anti-carcinomas Compounds by Targeting SFRP4 Through Molecular Modeling, Docking and Dynamic Simulation Studies. Curr Comput Aided Drug Des. 2018;14(2):160–73. https://doi.org/10.2174/1573409914666180112100122 PMID: 29332600

41. Volkamer A, Kuhn D, Grombacher T, Rippmann F, Rarey M. Combining global and local measures for structure-based druggability predictions. J Chem Inf Model. 2012;52(2):360–72. https://doi.org/10.1021/ci200454v PMID: 22148551

42. Guex N, Peitsch MC. SWISS-MODEL and the Swiss-PdbViewer: an environment for comparative protein modeling. Electrophoresis. 1997;18(15):2714–23. https://doi.org/10.1002/elps.1150181505 PMID: 9504803

43. Dallakyan S, Olson AJ. Small-molecule library screening by docking with PyRx. Chemical biology: methods and protocols. Springer. 2014. p. 243–50.

44. Dankwa B, Broni E, Enninful KS, Kwofie SK, Wilson MD. Consensus docking and MM-PBSA computations identify putative furin protease inhibitors for developing potential therapeutics against COVID-19. Struct Chem. 2022;33(6):2221–41. https://doi.org/10.1007/s11224-022-02056-1 PMID: 36118173

45. Kemmish H, Fasnacht M, Yan L. Fully automated antibody structure prediction using BIOVIA tools: Validation study. PLoS One. 2017;12(5):e0177923. https://doi.org/10.1371/journal.pone.0177923 PMID: 28542300

46. Systèmes D. Discovery studio modeling environment. San Diego, CA, USA: Dassault Systèmes Biovia; 2016.

47. Ghelichkhani S, Saffari-Chaleshtori J, Ghaffari F, Nili-Ahmadabadi A. The Cytotoxic Effect of Thymoquinone Enhance on HepG2 Cell Line due to Induction of Fenton Reaction by Hydrogen Peroxide: An In Vitro and In Silico Study. Asian Pac J Cancer Prev. 2023;24(5):1809–15. https://doi.org/10.31557/APJCP.2023.24.5.1809 PMID: 37247304

48. Chen J, Zeng Q, Wang W, Sun H, Hu G. Decoding the identification mechanism of an SAM-III riboswitch on ligands through multiple independent Gaussian-accelerated molecular dynamics simulations. Journal of Chemical Information and Modeling. 2022;62(23):6118–32.

49. Kumar S, Abbas F, Ali I, Gupta MK, Kumar S, Garg M. Integrated network pharmacology and in-silico approaches to decipher the pharmacological mechanism of Selaginella tamariscina in the treatment of non-small cell lung cancer. Phytomedicine Plus. 2023;3(2):100419.

50. Release S. Desmond molecular dynamics system. New York, NY: DE Shaw Research; 2017.

51. Bowers KJ, Chow E, Xu H, Dror RO, Eastwood MP, Gregersen BA, et al., editors. Scalable algorithms for molecular dynamics simulations on commodity clusters. Proceedings of the 2006 ACM/IEEE Conference on Supercomputing; 2006.

52. Bai J, Liu Z, Xu Z, Ke F, Zhang L, Zhu H, et al. Epigenetic downregulation of SFRP4 contributes to epidermal hyperplasia in psoriasis. J Immunol. 2015;194(9):4185–98. https://doi.org/10.4049/jimmunol.1403196 PMID: 25825452

53. Huang D, Yu B, Deng Y, Sheng W, Peng Z, Qin W, et al. SFRP4 was overexpressed in colorectal carcinoma. J Cancer Res Clin Oncol. 2010;136(3):395–401. https://doi.org/10.1007/s00432-009-0669-2 PMID: 19730886

54. Deshmukh A, Arfuso F, Newsholme P, Dharmarajan A. Epigenetic demethylation of sFRPs, with emphasis on sFRP4 activation, leading to Wnt signalling suppression and histone modifications in breast, prostate, and ovary cancer stem cells. Int J Biochem Cell Biol. 2019;109:23–32. https://doi.org/10.1016/j.biocel.2019.01.016 PMID: 30710752

55. Wu Q, Xu C, Zeng X, Zhang Z, Yang B, Rao Z. Tumor suppressor role of sFRP-4 in hepatocellular carcinoma via the Wnt/β-catenin signaling pathway. Mol Med Rep. 2021;23(5):336. https://doi.org/10.3892/mmr.2021.11975 PMID: 33760186

56. Busuttil RA, George J, House CM, Lade S, Mitchell C, Di Costanzo NS, et al. SFRP4 drives invasion in gastric cancer and is an early predictor of recurrence. Gastric Cancer. 2021;24(3):589–601. https://doi.org/10.1007/s10120-020-01143-8 PMID: 33277667

57. Han X, Saiyin H, Zhao J, Fang Y, Rong Y, Shi C. Overexpression of miR-135b-5p promotes unfavorable clinical characteristics and poor prognosis via the repression of SFRP4 in pancreatic cancer. Oncotarget. 2017;8(37):62195.

58. Mandal S, Gamit N, Varier L, Dharmarajan A, Warrier S. Inhibition of breast cancer stem-like cells by a triterpenoid, ursolic acid, via activation of Wnt antagonist, sFRP4 and suppression of miRNA-499a-5p. Life Sci. 2021;265:118854. https://doi.org/10.1016/j.lfs.2020.118854 PMID: 33278391

59. Özel Yetkin M, Baskol G. Silibinin reduces cell proliferation and migration via EMT pathway in TFK-1 cell line. Turkish Journal of Biochemistry. 2024;48(6):709–17.

60. Lashgarian HE, Adamii V, Ghorbanzadeh V, Chodari L, Kamali F, Akbari S, et al. Silibinin Inhibit Cell Migration through Downregulation of RAC1 Gene Expression in Highly Metastatic Breast Cancer Cell Line. Drug Res (Stuttg). 2020;70(10):478–83. https://doi.org/10.1055/a-1223-1734 PMID: 32791535

61. Mokhtari MJ, Motamed N, Shokrgozar MA. Evaluation of silibinin on the viability, migration and adhesion of the human prostate adenocarcinoma (PC-3) cell line. Cell Biol Int. 2008;32(8):888–92. https://doi.org/10.1016/j.cellbi.2008.03.019 PMID: 18538589

62. Barros TM, Lima AP, Almeida TC, da Silva GN. Inhibition of urinary bladder cancer cell proliferation by silibinin. Environmental and Molecular Mutagenesis. 2020;61(4):445–55.

63. Toma S, Isnardi L, Raffo P, Dastoli G, De Francisci E, Riccardi L. Effects of ALL-trans-retinoic acid and 13-cis-retinoic acid on breast-cancer cell lines: Growth inhibition and apoptosis induction. International Journal of Cancer. 1997;70(5):619–27.

64. Bhal S, Kundu CN. Targeting crosstalk of signaling pathways in cancer stem cells: a promising approach for development of novel anti-cancer therapeutics. Med Oncol. 2023;40(2):82. https://doi.org/10.1007/s12032-022-01905-7 PMID: 36662310

65. Firouzi J, Sotoodehnejadnematalahi F, Shokouhifar A, Rahimi M, Sodeifi N, Sahranavardfar P, et al. Silibinin exhibits anti-tumor effects in a breast cancer stem cell model by targeting stemness and induction of differentiation and apoptosis. Bioimpacts. 2022;12(5):415–29. https://doi.org/10.34172/bi.2022.23336 PMID: 36381630

66. Tolosa L, Donato MT, Gómez-Lechón MJ. General cytotoxicity assessment by means of the MTT assay. Protocols in in vitro hepatocyte research. Springer; 2014. p. 333–48.

67. Si L, Fu J, Liu W, Hayashi T, Nie Y, Mizuno K, et al. Silibinin inhibits migration and invasion of breast cancer MDA-MB-231 cells through induction of mitochondrial fusion. Mol Cell Biochem. 2020;463(1–2):189–201. https://doi.org/10.1007/s11010-019-03640-6 PMID: 31612353

68. Hossein-Tehrani M, Abbasalipourkabir R, Ziamajidi N. The role of miR-133a in silibinin-mediated inhibition of the PI3K/AKT/mTOR pathway in MCF-7 breast carcinoma cells. Mol Biol Res Commun. 2024;13(2):79–83. https://doi.org/10.22099/MBRC.2024.48818.1903 PMID: 38504785

69. Kil WH, Kim SM, Lee JE, Park KS, Nam SJ. Anticancer effect of silibinin on the xenograft model using MDA-MB-468 breast cancer cells. Ann Surg Treat Res. 2014;87(4):167–73. https://doi.org/10.4174/astr.2014.87.4.167 PMID: 25317410

70. Wang B, Yan Y, Zhou J, Zhou Q, Gui S, Wang Y. A novel all-trans retinoid acid derivatives inhibits the migration of breast cancer cell lines MDA-MB-231 via myosin light chain kinase involving p38-MAPK pathway. Biomed Pharmacother. 2013;67(5):357–62. https://doi.org/10.1016/j.biopha.2013.03.016 PMID: 23602051

71. Khramtsov AI, Khramtsova GF, Tretiakova M, Huo D, Olopade OI, Goss KH. Wnt/beta-catenin pathway activation is enriched in basal-like breast cancers and predicts poor outcome. Am J Pathol. 2010;176(6):2911–20. https://doi.org/10.2353/ajpath.2010.091125 PMID: 20395444

72. Geyer FC, Lacroix-Triki M, Savage K, Arnedos M, Lambros MB, MacKay A, et al. β-Catenin pathway activation in breast cancer is associated with triple-negative phenotype but not with CTNNB1 mutation. Mod Pathol. 2011;24(2):209–31. https://doi.org/10.1038/modpathol.2010.205 PMID: 21076461

73. Fu J, Liu W, Liu S, Zhao R, Hayashi T, Zhao H, et al. Inhibition of YAP/TAZ pathway contributes to the cytotoxicity of silibinin in MCF-7 and MDA-MB-231 human breast cancer cells. Cell Signal. 2024;119:111186. https://doi.org/10.1016/j.cellsig.2024.111186 PMID: 38643945

74. Gnanamathy G, Jeevitha R, Elumalai P, Sridevi M. Silibinin induces apoptosis and suppresses cell migration by targeting the transforming growth factor-β signaling pathway in osteosarcoma cells. 2024.

75. Ray PP, Islam MA, Islam MS, Han A, Geng P, Aziz MA, et al. A comprehensive evaluation of the therapeutic potential of silibinin: a ray of hope in cancer treatment. Front Pharmacol. 2024;15:1349745. https://doi.org/10.3389/fphar.2024.1349745 PMID: 38487172

76. Al-Hajj M, Wicha MS, Benito-Hernandez A, Morrison SJ, Clarke MF. Prospective identification of tumorigenic breast cancer cells. Proc Natl Acad Sci U S A. 2003;100(7):3983–8. https://doi.org/10.1073/pnas.0530291100 PMID: 12629218

77. Ginestier C, Hur MH, Charafe-Jauffret E, Monville F, Dutcher J, Brown M, et al. ALDH1 is a marker of normal and malignant human mammary stem cells and a predictor of poor clinical outcome. Cell Stem Cell. 2007;1(5):555–67. https://doi.org/10.1016/j.stem.2007.08.014 PMID: 18371393

78. Saliu TP, Seneviratne NN, Faizan M, Rajagopalan U, Perera DC, Adhikari A, et al. In silico identification and in vitro validation of alpha-hederin as a potent inhibitor of Wnt/β-catenin signaling pathway in breast cancer stem cells. In Silico Pharmacol. 2024;12(1):31. https://doi.org/10.1007/s40203-024-00199-z PMID: 38617708